Diagrammatic determinantal quantum Monte Carlo methods: Projective schemes and applications to the Hubbard-Holstein model

F. F. Assaad and T. C. Lang

Institut für Theoretische Physik und Astrophysik, Universität Würzburg, Am Hubland, D-97074 Würzburg, Germany

We extend the weak-coupling diagrammatic determinantal algorithm to projective schemes as well as to the inclusion of phonon degrees of freedom. The projective approach provides a very efficient algorithm to access zero-temperature properties. To implement phonons, we integrate them out in favor of a retarded density-density interaction and simulate the resulting purely electronic action with the weak-coupling diagrammatic determinantal algorithm. Both extensions are tested within the dynamical mean-field approximation for the Hubbard and Hubbard-Holstein models.

PACS number(s): 71.27.+a, 71.10.−w, 71.10.Fd

I. INTRODUCTION

Diagrammatic determinantal quantum Monte Carlo (DDQMC), be it the weak-coupling expansion[1] or hybridization expansion[2] approach, is emerging as the method of choice for impurity solvers.[3] In comparison to the Hirsch-Fye approach,[4] it uses continuous time methods and is thereby free of Trotter errors, is more efficient, and more flexible. In this paper, we concentrate on the weak-coupling algorithm. After a short review of our implementation of the algorithm, we show how to generalize it to projective schemes as well as to the inclusion of phonon degrees of freedom.

Projective schemes have already been implemented in the framework of the Hirsch-Fye algorithm and used in the context of dynamical mean-field theories.[5–7] Very similar ideas for the formulation of a projective DDQMC algorithm may be used and are reviewed in Sec. III. With the projective DDQMC, we can reproduce results of Ref. 5 at a fraction of the computational cost and access much lower projection parameters.

Phonon degrees of freedom have very recently been implemented in the strong coupling formulation of the DDQMC.[8] Since the strong-coupling approach is based on the expansion in the hybridization, the inclusion of phonons relies on a Lang-Firsov transformation. In the weak-coupling approach, it is more convenient to integrate out the phonons in favor of a retarded interaction. The purely electronic model may then be solved efficiently within the weak-coupling DDQMC. In Sec. IV, we present some details of the algorithm and provide test simulations for the Hubbard-Holstein model in the dynamical mean-field theory (DMFT) approximation.

II. DIAGRAMMATIC DETERMINANTAL METHOD FOR HUBBARD INTERACTIONS

Here, we will briefly review the diagrammatic determinantal method for the Hubbard model

$$\hat{H}_U = -\underbrace{\sum_{i,j,\sigma} t_{i,j}\hat{c}_{i,\sigma}^\dagger \hat{c}_{j,\sigma}}_{\hat{H}_0} + U\sum_i \left(\hat{n}_{i,\uparrow}-\frac{1}{2}\right)\left(\hat{n}_{i,\downarrow}-\frac{1}{2}\right), \tag{1}$$

where $\hat{n}_{i,\sigma}=\hat{c}_{i,\sigma}^\dagger \hat{c}_{i,\sigma}$, and $\hat{c}_{i,\sigma}^\dagger$ ($\hat{c}_{i,\sigma}$) creates (annihilates) a fermion in a Wannier state centered around site i (j) and with z component of spin σ.

As will become apparent in subsequent sections, we rewrite the Hubbard interaction as

$$\frac{U}{2}\sum_i \sum_{s=\pm 1}\left(\hat{n}_{i,\uparrow}-\frac{1}{2}-s\delta\right)\left(\hat{n}_{i,\downarrow}-\frac{1}{2}+s\delta\right) \tag{2}$$

to avoid the negative sign problem, at least for impurity and one-dimensional models. After carrying out the sum over the Ising spins, s, one recovers the original Hubbard interaction up to a constant. As will be seen below, an adequate choice of δ to avoid the sign problem for a one-dimensional chain reads $\delta=\frac{1}{2}+0^+$.

A weak-coupling perturbation expansion yields for the partition function:

$$\frac{Z}{Z_0} = \sum_{n=0}^\infty \left(\frac{-U}{2}\right)^n \int_0^\beta d\tau_1 \sum_{i_1,s_1} \cdots \int_0^{\tau_{n-1}} d\tau_n$$
$$\times \sum_{i_n,s_n}\prod_\sigma \langle[\hat{n}_{i_1,\sigma}(\tau_1)-\alpha_\sigma(s_1)]\cdots[\hat{n}_{i_n,\sigma}(\tau_n)-\alpha_\sigma(s_n)]\rangle_0. \tag{3}$$

Here, we have defined

$$\alpha_\sigma(s) = 1/2 + \sigma s\delta \tag{4}$$

and $\langle\bullet\rangle_0=\text{Tr}[e^{-\beta\hat{H}_0}\bullet]/Z_0$ with $Z_0=\text{Tr}[e^{-\beta\hat{H}_0}]$. Note that the Ising field s has obtained an additional time index. The thermal expectation value is the sum over all diagrams, connected and disconnected, of a given order n. Using Wick's theorem, this sum can be expressed as a determinant where the entries are the Green's functions of the noninteracting system.

$$\langle T[\hat{n}_{\sigma,i_1}(\tau_1) - \alpha_\sigma(s_1)] \cdots [\hat{n}_{\sigma,i_n}(\tau_n) - \alpha_\sigma(s_n)] \rangle_0 = \det \begin{pmatrix} G^0_{i_1,i_1}(\tau_1,\tau_1) - \alpha_\sigma(s_1) & G^0_{i_1,i_2}(\tau_1,\tau_2) & \cdots & G^0_{i_1,i_n}(\tau_1,\tau_n) \\ G^0_{i_2,i_1}(\tau_2,\tau_1) & G^0_{i_2,i_2}(\tau_2,\tau_2) - \alpha_\sigma(s_2) & \cdots & G^0_{i_2,i_n}(\tau_2,\tau_n) \\ \vdots & \vdots & \vdots & \vdots \\ G^0_{i_n,i_1}(\tau_n,\tau_1) & G^0_{i_n,i_2}(\tau_n,\tau_2) & \cdots & G^0_{i_n,i_n}(\tau_n,\tau_n) - \alpha_\sigma(s_n) \end{pmatrix},$$

$$(5)$$

with Green's functions

$$G^0_{i,j}(\tau_1,\tau_2) = \langle T\hat{c}^\dagger_i(\tau_1)\hat{c}_j(\tau_2) \rangle_0, \tag{6}$$

which we have assumed to be spin independent. In the above, T corresponds to the time ordering. Defining a configuration C_n by the n Hubbard vertices, as well as the Ising spins introduced in Eq. (2)

$$C_n = \{[i_1,\tau_1,s_1] \cdots [i_n,\tau_n,s_n]\}, \tag{7}$$

and the *sum* over the configuration space by

$$\sum_{C_n} = \sum_{n=0}^{\infty} \int_0^\beta d\tau_1 \sum_{i_1,s_1} \cdots \int_0^{\tau_{n-1}} d\tau_n \sum_{i_n,s_n}, \tag{8}$$

the partition function can conveniently be written as

$$\frac{Z}{Z_0} = \sum_{C_n} \left(-\frac{U}{2}\right)^n \prod_\sigma \det M_\sigma(C_n). \tag{9}$$

Here, M_σ is the $n \times n$ matrix of Eq. (5). Observables, $\hat{O}(\tau)$, can now be computed with

$$\langle \hat{O}(\tau) \rangle = \frac{\displaystyle\sum_{C_n} \left(-\frac{U}{2}\right)^n \prod_\sigma \det M_\sigma(C_n) \langle\langle \hat{O}(\tau) \rangle\rangle_{C_n}}{\displaystyle\sum_{C_n} \left(-\frac{U}{2}\right)^n \prod_\sigma \det M_\sigma(C_n)}, \tag{10}$$

where for $\hat{O}(\tau) = \Pi_\sigma \hat{O}_\sigma(\tau)$ we have

$$\langle\langle \hat{O}(\tau) \rangle\rangle_{C_n} = \frac{\displaystyle\prod_\sigma \langle T[\hat{n}_{i_1,\sigma}(\tau_1) - \alpha_\sigma(s_1)] \cdots [\hat{n}_{i_n,\sigma}(\tau_n) - \alpha_\sigma(s_n)]\hat{O}_\sigma(\tau) \rangle_0}{\displaystyle\prod_\sigma \langle T[\hat{n}_{i_1,\sigma}(\tau_1) - \alpha_\sigma(s_1)] \cdots [\hat{n}_{i_n,\sigma}(\tau_n) - \alpha_\sigma(s_n)] \rangle_0}. \tag{11}$$

For any given configuration of vertices C_n, Wick's theorem holds. Hence, any observable can be computed from the knowledge of the single particle Green's function

$$\langle\langle T c^\dagger_{i,\sigma}(\tau)c_{j,\sigma}(\tau_1) \rangle\rangle_{C_n}$$

$$= G^0_{i,j}(\tau,\tau_1) - \sum_{r,s=1}^n G^0_{i,i_r}(\tau,\tau_{i_r})(M^{-1}_\sigma)_{r,s} G^0_{i_s,j}(\tau_s,\tau_1). \tag{12}$$

Here, we have assumed that the noninteracting Green's functions are spin independent. As a consequence of the above equation, it becomes apparent that one can measure directly the Matsubara Green's functions. This aspect facilitates the implementation of the algorithm within the framework of dynamical mean-field theories.

A. Sign problem

In auxiliary field determinantal methods,[9] it is known that the presence of particle-hole symmetry can be used to avoid

the negative sign problem. An identical statement holds for the diagrammatic determinantal method. We assume that $\hat{H}_0$ is invariant under the particle-hole transformation

$$c^\dagger_{i,\sigma} \rightarrow (-1)^i c_{i,\sigma}. \tag{13}$$

As a consequence,

$$\left\langle T\prod_{r=1}^n n[\hat{n}_{i_r,\sigma}(\tau_r) - \alpha_\sigma(s_r)] \right\rangle_0$$

$$= (-1)^n \left\langle T\prod_{r=1}^n n[\hat{n}_{i_r,\sigma}(\tau_r) - \alpha_{-\sigma}(s_r)] \right\rangle_0 \tag{14}$$

such that $\det M_\uparrow = (-1)^n \det M_\downarrow$. A glimpse at Eq. (9) will confirm the absence of a sign problem for this special case. The above result is independent of the choice of δ introduced in Eq. (2). As we will see in Sec. II C, the algorithm is optimal at $\delta = 0$. In this special case, $\det M_\uparrow = \det M_\downarrow = (-1)^n \det M_\downarrow$ such that only even values of n occur in the sampling. We note that this vanishing of the weight for odd

values of n can be avoided by choosing a small value of δ.

In one dimension and in the absence of frustrating interactions, there is no negative sign problem.[15] The diagrammatic approach also satisfies this property, provided that we choose $\delta = 1/2 + 0^+$. The quantity $\Pi_\sigma \det M_\sigma(C_n)$ in Eq. (9) is nothing but

$$\text{Tr}\left[e^{-\beta \hat{H}_0} \prod_\sigma [\hat{n}_{i_1,\sigma}(\tau_1) - \alpha_\sigma(s_1)] \cdots \right. $$
$$\left. \times [\hat{n}_{i_n,\sigma}(\tau_n) - \alpha_\sigma(s_n)] \right] \Big/ \text{Tr}[e^{-\beta \hat{H}_0}], \quad (15)$$

which we can compute within the real-space world-line approach.[10,11] Here, each world-line configuration has a positive weight. Let us consider an arbitrary world-line configuration, and a site (i, τ) in the space-time lattice. Irrespective if this site is empty, singly, or doubly occupied, the expectation value of the operator $\Pi_\sigma[\hat{n}_{i,\sigma}(\tau) - \alpha_\sigma(s)]$ will take a negative value. Recall that we have set $\delta = 1/2 + 0^+$. Hence, for each world-line configuration, the expectation value of the operator $\Pi_\sigma[(\hat{n}_{i,\sigma}(\tau) - \alpha_\sigma(s_1)) \cdots (\hat{n}_{i_n,\sigma}(\tau_n) - \alpha_\sigma(s_n))]$ has a sign equal to $(-1)^n$. Summation over all world-line configurations yields the expression in Eq. (15), which in turn has a sign $(-1)^n$. This cancels the sign of the factor $(-U/2)^n$ in Eq. (9), thus yielding an overall positive weight.

In the rewriting of the Hubbard term [see Eq. (2)], we have introduced a dynamical Ising field so as to avoid the negative sign problem, at least for the one-dimensional Hubbard model. Alternatively, one can choose a static Ising field and compensate for it by a redefinition of $\hat{H}_0$. Such a static procedure is introduced in Ref. 1. For the class of models considered, we have not noticed substantial differences in performance between static and dynamical choices of Ising fields. We, however, favor the dynamical version since it allows one to keep the SU(2) spin invariant form of the noninteracting Hamiltonian $\hat{H}_0$.

B. Monte Carlo sampling

In principle, two moves, the addition and removal of Hubbard vertices, are sufficient.[16] In the Metropolis scheme, the acceptance ratio for a given move reads

$$P_{C \to C'} = \min\left(\frac{T^0_{C' \to C} W(C')}{T^0_{C \to C'} W(C)}, 1 \right), \quad (16)$$

where $T^0_{C' \to C}$ corresponds to the probability of proposing a move from configuration C' to configuration C, and $W(C)$ corresponds to the weight of the configuration. To add a vertex $T^0_{C_n \to C_{n+1}} = \frac{1}{2N\beta}$ corresponds to the fact that one has to pick at random an imaginary time in the range $[0, \beta]$, a site i in the range $1, \ldots, N$ (with N the number of sites), and an Ising spin. The proposal probability to remove a vertex $T^0_{C_{n+1} \to C_n} = \frac{1}{n+1}$ corresponds to the fact that one will choose at random one of the $n+1$ vertices present in configuration C_{n+1}, hence

$$P_{C_n \to C_{n+1}} = \min\left(-\frac{U\beta N}{(n+1)} \frac{\prod_\sigma \det M_\sigma(C_{n+1})}{\prod_\sigma \det M_\sigma(C_n)}, 1 \right),$$

$$P_{C_{n+1} \to C_n} = \min\left(-\frac{(n+1)}{U\beta N} \frac{\prod_\sigma \det M_\sigma(C_n)}{\prod_\sigma \det M_\sigma(C_{n+1})}, 1 \right). \quad (17)$$

Apart from the above addition and removal of vertices, we have implemented moves which flip the Ising spins at constant order n as well as updates which move Hubbard vertices both in space and time.

C. Tests

The efficiency of the approach relies on the autocorrelation time, which has to be analyzed on a case to case basis, as well as on the average expansion order parameter. For a general interaction term $\hat{H}_1$, the average expansion parameter is given by

$$\langle n \rangle = \frac{1}{Z} \sum_n \frac{(-1)^n n}{n!} \int_0^\beta d\tau_1 \cdots \int_0^\beta d\tau_n \langle T\hat{H}_1(\tau_1) \cdots \hat{H}_1(\tau_n) \rangle_0$$

$$= \frac{-1}{Z} \sum_m \frac{(-1)^m}{m!} \int_0^\beta d\tau_1 \cdots$$

$$\times \int_0^\beta d\tau_m \int_0^\beta d\tau \langle T\hat{H}_1(\tau_1) \cdots \hat{H}_1(\tau_m) \hat{H}_1(\tau) \rangle_0$$

$$= -\int_0^\beta d\tau \langle \hat{H}_1(\tau) \rangle. \quad (18)$$

For the Hubbard model and replacing $\hat{H}_1$ by the form of Eq. (2), we obtain

$$\langle n \rangle = -\beta U \sum_i \left[\left\langle \left(\hat{n}_{i,\uparrow} - \frac{1}{2} \right) \left(\hat{n}_{i,\downarrow} - \frac{1}{2} \right) \right\rangle - \delta^2 \right]. \quad (19)$$

Using the same techniques as in auxiliary field quantum Monte Carlo methods,[9] the CPU costs for the calculation of the acceptance probability and the update for the addition or removal of a vertex scales as n^2. As apparent from Eq. (19), a sweep consisting of updating all n vertices results in an effort of n^3. Even though in this method M_σ^{-1} is far better conditioned than in the *classic* determinantal methods,[4,9,12] it has to be recalculated from scratch after several updates, which involves an effort of the order n^3.[17] Hence, because of these two limiting factors, the CPU time scales as $(\beta UN)^3$, which is precisely the same scaling as in the Hirsch-Fye approach. Apart from the absence of Trotter errors, the advantage of the method lies in a large prefactor. In the very special case of a single impurity, $N=1$, and for a particle-hole symmetric Hamiltonian $\hat{H}_0$, the speedup is dramatic. Particle-hole symmetry allows one to set $\delta = 0$ such that $\langle n \rangle < \beta U/4$. To obtain this upper bound, we have set the double occupancy to zero. Hence a simulation at $U/t = 4$ and βt

=400 has a maximal average order parameter $\langle n \rangle = 400$. In a Hirsch-Fye approach, one could opt for a Trotter step $\Delta \tau = 1/8$ and hence 3200 Trotter slices, which determine the size of the matrices involved in the simulations. Hence an underestimate of the speedup reads $(3200/400)^3 = 512$. Away from particle-hole symmetry, the speedup is less impressive since we have to set $\delta = 1/2 + 0^+$ to avoid the negative sign problem. We have confirmed the above statements for the Anderson impurity model,

$$\hat{H} = \sum_{k,\sigma} [\epsilon(k) - \mu] \hat{c}_{k,\sigma}^\dagger \hat{c}_{k,\sigma} + \frac{V}{\sqrt{N}} \sum_{k,\sigma} (\hat{c}_{k,\sigma}^\dagger \hat{d}_\sigma + \text{H.c.})$$

$$+ U \left(\hat{d}_\uparrow^\dagger \hat{d}_\uparrow - \frac{1}{2} \right) \left(\hat{d}_\downarrow^\dagger \hat{d}_\downarrow - \frac{1}{2} \right), \tag{20}$$

with Hubbard interaction U and hybridization V. Here, $\hat{c}_{k,\sigma}^\dagger$ ($\hat{c}_{k,\sigma}$) creates (annihilates) a fermion in the conduction band at momentum k with spin σ and the dispersion relation $\epsilon(k) = -2t[\cos(k_x) + \cos(k_y)]$. The operators $\hat{d}_\sigma^\dagger$ and $\hat{d}_\sigma$ create and annihilate an impurity electron, respectively. Our results including comparison with the Hirsch-Fye algorithm are presented in Fig. 1.

Finally, let us note that applying the method to a one-dimensional Hubbard model of length N yields a very poor performance in comparison to standard finite temperature Blancenbecler-Scalapino-Sugar (BSS) auxiliary field algorithms[12] since those methods scale as $\beta U N^3$.[9]

III. GENERALIZATION TO PROJECTIVE APPROACHES

Projective approaches rely on the filtering out of the ground state $|\Psi_0\rangle$ from a trial wave function $|\Psi_T\rangle$, which is required to be nonorthogonal to $|\Psi_0\rangle$

$$\frac{\langle \Psi_0 | \hat{O} | \Psi_0 \rangle}{\langle \Psi_0 | \Psi_0 \rangle} = \lim_{\Theta \to \infty} \frac{\langle \Psi_T | e^{-(\Theta/2)\hat{H}} \hat{O} e^{-(\Theta/2)\hat{H}} | \Psi_T \rangle}{\langle \Psi_T | e^{-\Theta \hat{H}} | \Psi_T \rangle}. \tag{21}$$

For convenience and simplicity, we will assume that $|\Psi_T\rangle$ is the ground state of $\hat{H}_0$, such that for a given value of Θ the right hand side of the above equation can be written as

$$\frac{\langle \Psi_T | e^{-(\Theta/2)\hat{H}} \hat{O} e^{-(\Theta/2)\hat{H}} | \Psi_T \rangle}{\langle \Psi_T | e^{-\Theta \hat{H}} | \Psi_T \rangle} = \lim_{\beta_0 \to \infty} \frac{\text{Tr } e^{-\beta_0 \hat{H}_0} e^{-(\Theta/2)\hat{H}} \hat{O} e^{-(\Theta/2)\hat{H}}}{\text{Tr } e^{-\beta_0 \hat{H}_0} e^{-\Theta \hat{H}}}. \tag{22}$$

With the definition $Z_p = \text{Tr}[e^{-\beta_0 \hat{H}_0} e^{-\Theta \hat{H}}]$ and $Z_{p,0} = \text{Tr}[e^{-(\beta_0 + \Theta)\hat{H}_0}]$, a weak-coupling expansion yields

$$\frac{Z_p}{Z_{p,0}} = \sum_{n=0}^\infty \left(\frac{-U}{2} \right)^n \int_0^\Theta d\tau_1 \sum_{i_1, s_1} \cdots \int_0^{\tau_{n-1}} d\tau_n$$

$$\times \sum_{i_n, s_n} \prod_\sigma \langle [\hat{n}_{i_1,\sigma}(\tau_1) - \alpha_\sigma(s_1)] \cdots$$

$$\times [\hat{n}_{i_n,\sigma}(\tau_n) - \alpha_\sigma(s_n)] \rangle_{p,0}, \tag{23}$$

where $\langle \bullet \rangle_{p,0} = \text{Tr}[e^{-(\beta_0 + \Theta)\hat{H}_0} \bullet]/Z_{p,0}$. The similarity to the finite
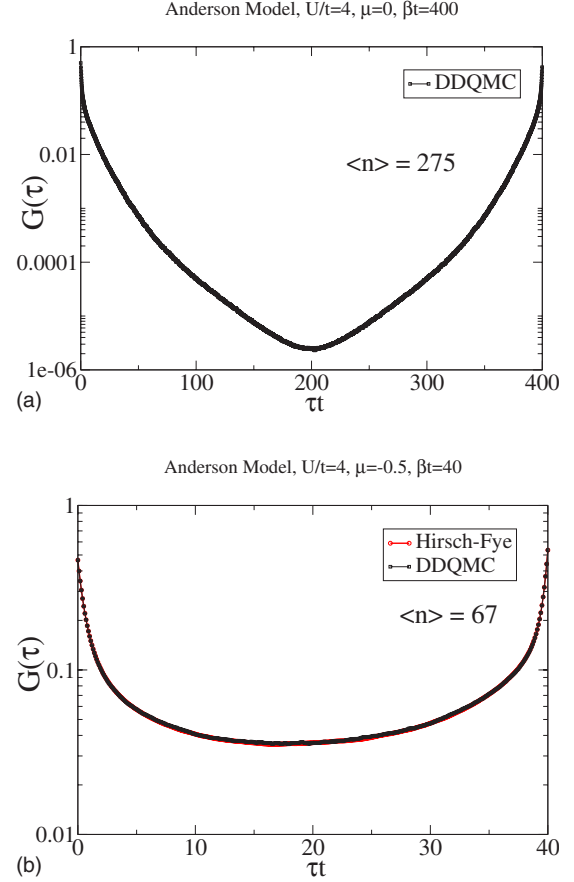

FIG. 1. (Color online) Green's function $G(\tau)$ for the Anderson model of Eq. (20). (a) Particle-hole symmetric point, $\mu = 0$. To avoid the vanishing of the weight at odd values of n, we have used $\delta = 0.1$ for this simulation. (b) Away from particle-hole symmetry, $\mu = -0.5$. For this higher temperature, we provide a comparison with the Hirsch-Fye algorithm with Trotter step $\Delta \tau = 0.1$. Note that in both cases we have used a 32×32 square lattice to generate the noninteracting Green's function $G^0(\tau)$. $\langle n \rangle$ corresponds to the average order expansion parameter.

temperature algorithm is now apparent. We use Wick's theorem to express the expectation value on the right hand side of Eq. (23) in terms of the product of two determinants. Taking the limit $\beta_0 \to \infty$, we obtain

$$\langle \Psi_T | e^{-\Theta \hat{H}} | \Psi_T \rangle \equiv \lim_{\beta_0 \to \infty} \frac{Z_p}{Z_{p,0}} = \sum_{C_n} \left(-\frac{U}{2} \right)^n \prod_\sigma \det M_{\sigma,p}(C_n). \tag{24}$$

Here, the sum runs over all configurations C_n as defined in Eqs. (7) and (8). Note that β in Eq. (8) has to be replaced by Θ. The matrices $M_{\sigma,p}$ have precisely the same form as the matrices M_σ, but since we have taken the limit $\beta_0 \to \infty$, the thermal noninteracting Green's functions have to be replaced by the zero-temperature ones:

$$G_{p,i,j}^0(\tau_1, \tau_2) = \langle \Psi_T | T \hat{c}_i^\dagger(\tau_1) \hat{c}_j(\tau_2) | \Psi_T \rangle. \tag{25}$$

Hence, as in the Hirsch-Fye approach, the step from a finite temperature to zero-temperature code is very easy and essen-
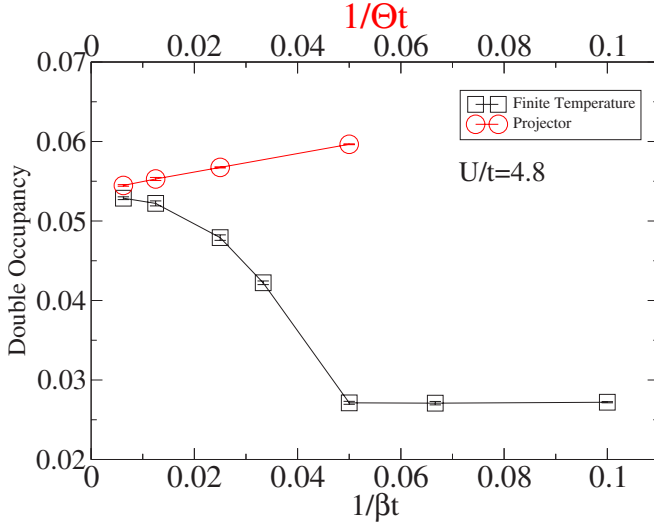
FIG. 2. (Color online) DMFT calculation of the double occupancy for the half filled Hubbard model as a function of (i) temperature $1/\beta$ and (ii) projection parameter $1/\Theta$. In the projective approach, observables are computed in the imaginary time range $[\Theta/4, 3\Theta/4]$. This rather large measurement interval explains the slight discrepancy with the data of Ref. 5 for the projective code and at finite values of Θ. However, extrapolation to $\Theta \to \infty$, where the measurement range becomes irrelevant, yields results consistent with Ref. 5.

tially amounts in replacing the finite temperature noninteracting Green's functions by the zero-temperature ones. However, there is an important difference concerning measurements: measurements of observables which do not commute with the Hamiltonian have to be carried out in the middle of the imaginary time interval $[0, \Theta]$ to avoid boundary effects.[9] We have tested this approach by reproducing Fig. 1 of Ref. 5, where the projective Hirsch-Fye algorithm was incorporated in the DMFT self-consistency cycle. Figure 2 shows the results for the half filled Hubbard model at $U/t = 4.8$, density of states $N(\omega) = \frac{8}{\pi W^2}\sqrt{W^2/4 - \omega^2}$, and bandwidth $W = 4t$. Excellent agreement with the former Hirsch-Fye based results[5] both at finite temperatures and in the limit $\Theta \to \infty$ were obtained. However, the diagrammatic approach allows one to access much larger projection parameters and/or lower temperatures. We refer the reader to Ref. 5 for the implementation of the projective formalism in the self-consistency cycle.

IV. APPLICATION TO THE HUBBARD-HOLSTEIN MODEL

Weak-coupling DDQMC allows a very simple inclusion of phonon degrees of freedom. The path we follow here is to integrate out the phonons in favor of a retarded interaction, and then solve the purely electronic model with the DDQMC approach. Starting from the Hubbard-Holstein model with Einstein phonons, we show how to integrate out the phonons, describe some details of the algorithm, and then present results within the DMFT approximation.

A. Integrating out the phonons

The Hubbard-Holstein Hamiltonian we consider reads

$$\hat{H} = -\sum_{i,j,\sigma} t_{i,j}\hat{c}_{i,\sigma}^{\dagger}\hat{c}_{j,\sigma} + U\sum_i \left(\hat{n}_{i,\uparrow} - \frac{1}{2}\right)\left(\hat{n}_{i,\downarrow} - \frac{1}{2}\right)$$

$$+ g\sum_i \hat{Q}_i(\hat{n}_i - 1) + \sum_i \frac{\hat{P}_i^2}{2M} + \frac{k}{2}\hat{Q}_i^2. \tag{26}$$

Here, $\hat{n}_i = \sum_\sigma \hat{n}_{i,\sigma}$, and the last two terms correspond respectively to the electron-phonon coupling g and the phonon energy. The Hamiltonian is written such that for a particle-hole symmetric band, half filling corresponds to chemical potential $\mu = 0$. By opting for fermion coherent states

$$\hat{c}_{i,\sigma}|c\rangle = c_{i,\sigma}|c\rangle, \tag{27}$$

$c_{i,\sigma}$ being a Grassmann variable, and a real-space representation for the phonon coordinates

$$\hat{Q}_i|q\rangle = q_i|q\rangle, \tag{28}$$

the path integral formulation of the partition function reads

$$Z = \int [dq][dc^{\dagger}dc]e^{-(S_U + S_{ep})}, \tag{29}$$

with

$$S_U = \int_0^\beta d\tau \sum_{i,j,\sigma} c_{i,\sigma}^{\dagger}(\tau)\left(\delta_{i,j}\frac{\partial}{\partial\tau} - t_{i,j}\right)c_{j,\sigma}(\tau)$$

$$+ U\sum_i \left[n_{i,\uparrow}(\tau) - \frac{1}{2}\right]\left[n_{i,\downarrow}(\tau) - \frac{1}{2}\right],$$

$$S_{ep} = \int_0^\beta d\tau \sum_i \frac{M\dot{q}_i^2(\tau)}{2} + \frac{k}{2}q_i^2(\tau) + gq_i(\tau)[n_i(\tau) - 1]. \tag{30}$$

In Fourier space,

$$q_j(\tau) = \frac{1}{\sqrt{\beta N}}\sum_{k,\Omega_m} e^{-i(\Omega_m\tau - kj)}q_{k,m}, \tag{31}$$

where Ω_m is a bosonic Matsubara frequency; the electron-phonon part of the action reads

$$S_{ep} = \sum_{\Omega_m,k} \frac{M}{2}(\Omega_m^2 + \omega_0^2)q_{k,m}^{\dagger}q_{k,m} + gq_{k,m}\rho_{k,m}^{\dagger},$$

$$\rho_{k,m}^{\dagger} = \frac{1}{\sqrt{\beta N}}\int d\tau \sum_j e^{-i(\Omega_m\tau - kj)}[n_j(\tau) - 1]. \tag{32}$$

Gaussian integration over the phonon degrees of freedom leads to a retarded density-density interaction:

$$\int [dq] e^{-S_{ep}} = \exp\left\{ \int_0^\beta d\tau \int_0^\beta d\tau' \sum_{i,j} [n_i(\tau) - 1] \right.$$
$$\left. \times D^0(i-j, \tau-\tau')[n_j(\tau') - 1] \right\}. \quad (33)$$

For Einstein phonons, the phonon propagator is diagonal in real space,

$$D^0(i-j, \tau-\tau') = \delta_{i,j} \frac{g^2}{2k} P(\tau-\tau'),$$

$$P(\tau) = \frac{\omega_0}{2(1-e^{-\beta\omega_0})} (e^{-|\tau|\omega_0} + e^{-(\beta-|\tau|)\omega_0}). \quad (34)$$

Hence the partition function of the Hubbard-Holstein model takes the form

$$Z = \int [dc^\dagger dc] \exp\left\{ -\left(S_U - \int_0^\beta d\tau \int_0^\beta d\tau' \sum_{i,j} [n_i(\tau) - 1] \right. \right.$$
$$\left. \left. \times D^0(i-j, \tau-\tau')[n_j(\tau') - 1] \right) \right\}. \quad (35)$$

In the antiadiabatic limit, $\lim_{\omega_0 \to \infty} P(\tau) = \delta(\tau)$ such that the phonon interaction maps onto an attractive Hubbard interaction of magnitude g^2/k. We are now in a position to apply the DDQMC algorithm by expanding in both the retarded and Hubbard interactions.

B. Formulation of DDQMC for the Hubbard-Holstein model

To avoid the minus-sign problem at least for the one-dimensional chains, we rewrite the phonon retarded interaction as

$$H_P(\tau) = -\frac{g^2}{4k} \int_0^\beta d\tau' \sum_{i,\sigma,\sigma'} \sum_{s=\pm 1} P(\tau-\tau')[n_{i,\sigma}(\tau) - \alpha_+(s)]$$
$$\times [n_{i,\sigma'}(\tau') - \alpha_+(s)]. \quad (36)$$

For each phonon vertex, we have introduced an Ising variable s. Summation over this Ising field reproduces, up to a constant, the original interaction. Since the phonon term is attractive, the adequate choice of signs is $\alpha_+(s) \equiv 1/2 + s\delta$, irrespective of the spin σ and σ'. A similar argument as presented in Sec. II A then guarantees the absence of a sign problem for chains. Following Eq. (2) we rewrite the Hubbard term as

$$H_U(\tau) = \frac{U}{2} \sum_{i,s} \prod_\sigma [n_{i,\sigma}(\tau) - \alpha_\sigma(s)]. \quad (37)$$

To proceed with a description of the implementation of the algorithm, it is useful to define a general vertex

$$V(\tau) = \{i, \tau, \sigma, \tau', \sigma', s, b\}, \quad (38)$$

where b defines the type of vertex at hand, Hubbard ($b=0$) or phonon ($b=1$). For this vertex, we define a sum over the available phase

$$\sum_{V(\tau)} = \sum_{i,\sigma,\sigma',s,b} \int_0^\beta d\tau', \quad (39)$$

a *weight*

$$w[V(\tau)] = \delta_{b,0} \frac{U}{2} - \delta_{b,1} P(\tau-\tau') \frac{g^2}{4k}, \quad (40)$$

as well as

$$H[V(\tau)] = \delta_{b,0} \delta_{\sigma,\uparrow} \delta_{\sigma',\downarrow} \delta(\tau-\tau')$$
$$\times [n_{i,\uparrow}(\tau) - \alpha_+(s)][n_{i,\downarrow}(\tau) - \alpha_-(s)]$$
$$+ \delta_{b,1}[n_{i,\sigma}(\tau) - \alpha_+(s)][n_{i,\sigma'}(\tau') - \alpha_+(s)]. \quad (41)$$

With the above definitions, the partition function can now be written as

$$\frac{Z}{Z_0} = \sum_{n=0}^\infty (-1)^n \int_0^\beta d\tau_1 \sum_{V_1(\tau_1)} w[V_1(\tau_1)] \cdots \int_0^{\tau_{n-1}} d\tau_n$$
$$\times \sum_{V_n(\tau_n)} w[V_n(\tau_n)] \langle T\hat{H}[V_1(\tau_1)] \cdots \hat{H}[V_n(\tau_n)] \rangle_0. \quad (42)$$

As for the Hubbard model, a configuration consists of a set of vertices $C_n = \{V_1(\tau_1), \ldots, V_n(\tau_n)\}$. For a given configuration, the thermal expectation value maps onto the product of two determinants in the spin up and spin down sectors. The Monte Carlo sampling follows precisely the scheme presented in Sec. II B, namely, the addition and removal of vertices.

C. Application to the Hubbard-Holstein model in the dynamical mean-field approximation

We have applied the above algorithm to the Hubbard-Holstein model within the dynamical mean-field theory approximation. We use a semicircular density of states $N(\omega) = \frac{8}{\pi W^2} \sqrt{W^2/4 - \omega^2}$ with bandwidth $W = 4t$. Throughout this section, we set $U/t = 1$, $\omega_0 = 0.2t$, and $\mu = 0$, and use the finite temperature implementation of the algorithm at $\beta t = 40$. The choice $\mu = 0$ corresponds to half filling. Figure 3(a) plots the double occupancy, $D = \langle n_{i,\uparrow} n_{i,\downarrow} \rangle$, as a function of the electron-phonon coupling. To compare at best with the results of Ref. 13, we write the phonon coordinates in terms of bosonic operators, $\hat{Q} = \frac{1}{\sqrt{2M\omega_0}}(\hat{a} + \hat{a}^\dagger)$, and plot our results as a function of

$$\tilde{g} = g/\sqrt{2M\omega_0}. \quad (43)$$

Comparison of the results of Fig. 3(a) with those of Ref. 13 shows excellent agreement and a critical electron-phonon coupling for the transition to the bipolaronic insulator at $\tilde{g}_c \simeq 0.45t$.

We have equally computed the local spin and charge susceptibilities:
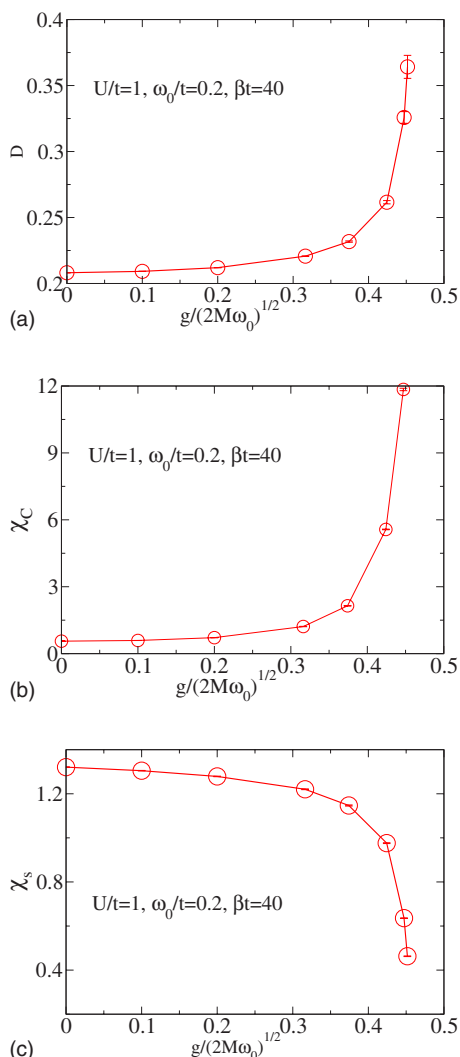
(a)

(b)

(c)

FIG. 3. (Color online) (a) Double occupancy, (b) local charge susceptibility, and (c) local spin susceptibility for the Hubbard-Holstein model in the DMFT approximation.

$$\chi_C^S = \int_0^\beta d\tau \langle [\hat{n}_{i,\uparrow}(\tau) \pm \hat{n}_{i,\downarrow}(\tau)][\hat{n}_{i,\uparrow} \pm \hat{n}_{i,\downarrow}]\rangle. \quad (44)$$

As can be seen in Fig. 3(b), in the vicinity the transition local charge fluctuations grow substantially and local spin fluctuations [see Fig. 3(c)] are suppressed. The suppression of χ_S signals singlet pairing of polarons. The chemical potential $\mu=0$ sets the average particle number $\rho=1$, but the particle number itself oscillates strongly between an empty or doubly
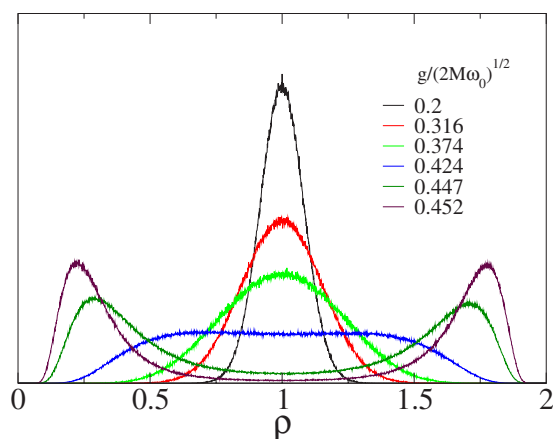

FIG. 4. (Color online) The normalized histogram of the local density ρ of the Hubbard-Holstein model at half filling with U/t =1, $\omega_0=0.2t$, and $\beta t=40$, for several values of the electron-phonon coupling g.

occupied site. This can be seen by taking histograms as shown in Fig. 4. In the vicinity of the transition, a two peak structure corresponding to a doubly occupied or empty site emerges. Close to the transition, it becomes increasingly hard to guarantee a symmetric histogram—corresponding to the particle-hole symmetry of the model—and the simulation ultimately freezes in the doubly occupied or empty state.

V. CONCLUSIONS

We have presented two extensions of the diagrammatic determinantal method: projective schemes as well as the inclusion of phonons. In both cases, we have tested successfully the approach for the Hubbard as well as for the Hubbard-Holstein models in the dynamical mean-field approximation. The inclusion of phonons is not limited to Einstein modes and, in principle, any dispersion relation can be easily implemented. Of the strong points of the weak-coupling DDQMC are that it can be extended very easily to larger clusters and used as a solver for cluster extensions of dynamical mean-field theories.[14] The crucial issue here is the severity of the sign problem as the cluster size increases. This is an issue which would need to be answered on a case to case basis.

[1] A. N. Rubtsov, V. V. Savkin, and A. I. Lichtenstein, Phys. Rev. B **72**, 035122 (2005).

[2] P. Werner, A. Comanac, L. deMedici, M. Troyer, and A. J. Millis, Phys. Rev. Lett. **97**, 076405 (2006).

[3] E. Gull, P. Werner, A. J. Millis, and M. Troyer, arXiv:cond-mat/0609438 (unpublished).

[4] J. E. Hirsch and R. M. Fye, Phys. Rev. Lett. **56**, 2521 (1986).

[5] M. Feldbacher, K. Held, and F. F. Assaad, Phys. Rev. Lett. **93**, 136405 (2004).

[6] M. I. Katsnelson, Phys. Rev. Lett. **96**, 139701 (2006).

[7] M. Feldbacher, K. Held, and F. F. Assaad, Phys. Rev. Lett. **96**, 139702 (2006).

[8] P. Werner and A. J. Millis, arXiv:cond-mat/0701730v2 (unpublished).

[9] F. F. Assaad, in *Lecture Notes of the Winter School on Quantum Simulations of Complex Many-Body Systems: From Theory to Algorithms*, edited by J. Grotendorst, D. Marx, and A. Muramatsu (von Neumann Institute for Computing, Jülich, 2002), Vol. 10, pp. 99–155.

[10] J. E. Hirsch, R. L. Sugar, D. J. Scalapino, and R. Blankenbecler, Phys. Rev. B **26**, 5033 (1982).

[11] F. F. Assaad and D. Würtz, Phys. Rev. B **44**, 2681 (1991).

[12] R. Blankenbecler, D. J. Scalapino, and R. L. Sugar, Phys. Rev. D **24**, 2278 (1981); D. J. Scalapino and R. L. Sugar, Phys. Rev. B **24**, 4295 (1981).

[13] W. Koller, D. Meyer, Y. Ono, and A. Hewson, Europhys. Lett. **66**, 559 (2004).

[14] T. Maier, M. Jarrell, T. Pruschke, and M. H. Hettler, Rev. Mod. Phys. **77**, 1027 (2005).

[15] To be more precise, configurations with negative weights do occur. However, those configurations stem from the real space winding of the fermions and can be eliminated if open boundary conditions are adopted.

[16] Clearly, those moves are not sufficient for the particle-hole symmetric case and $\delta=0$. In this case and as argued in Sec. II A, the weights vanish for odd values of n, and hence, the algorithm would not be ergodic. One can circumvent this problem by (i) introducing moves which add or remove pairs of vertices or (ii) using a small value of δ. For the simulations presented here, we have opted for solution (ii) and have chosen, in general, $\delta=0.1$ at the expense of a small performance loss.

[17] For the impurity problems presented here, M_σ^{-1} remains very stable, such that recalculation from scratch of M_σ^{-1} is not an issue. In contrast, when applying the method to a lattice problem, we find that round-off errors cumulate and a more frequent recalculation of M_σ^{-1} is required.